JOURNAL OF SOLID STATE CHEMISTRY 50, 138–145 (1983)

Infrared Studies on the Behavior in Oxygen of Cobalt-Substituted Magnetites: Comparison with Zinc-Substituted Magnetites

B. GILLOT AND F. JEMMALI

Laboratoire de Recherches sur la Réactivité des Solides, associé au CNRS Faculté des Sciences Mirande, B.P. 138, 21004 Dijon Cedex, France

AND A. ROUSSET

Laboratoire de Chimie des Matériaux Inorganiques, Université Paul Sabatier, Toulouse III, 118, route de Narbonne, 31000 Toulouse, France

Received April 11, 1983; in revised form June 20, 1983

Infrared spectroscopic measurements were carried out on the cobalt-substituted magnetites $(Fe^{3+})_A(Co_x^{2+}Fe_{1-x}^{2+}Fe^{3+})_BO_4^{2-}$, pretreated in oxygen, to investigate as a function of temperature the defect phases γ and their transformation to hematite. It has been found that the defect spinels for which $x < 0.30$ show a partial vacancy ordering on octahedral sites. Referring to the disappearance of the 720-cm^{-1} absorption band of the defect phases γ or the appearance of the 470-cm^{-1} absorption band of αFe_2O_3, we show that the transition temperature $\gamma \rightarrow \alpha$ increases with cobalt substitution. By comparison with zinc-substituted magnetites, the divalent cation distribution is shown to be important to vacancy ordering and to setting the temperature of hematite precipitation.

Introduction

In some earlier publications, the ir spectra of aluminum and chromium- or zinc-substituted magnetites and of the defect spinels resulting from their oxidation were described (*1, 2*). In the defect phases γ-$(Fe^{3+}_{(8-8y)/3}M^{3+}_{8y/3}\square_{1/3})O_4^{2-}$ with $0 < y < \frac{2}{3}$ and $M^{3+} = Cr^{3+}$, Al^{3+} or γ-$(Fe^{3+}_{(8-2x)/3}Zn_x^{2+}\square_{(1-x)/3})O_4^{2-}$ with $0 < x < 1$, a large number of well-defined absorption bands occur in the region 200–750 cm^{-1} in the low substitution range ($y < 0.26$ and $x < 0.30$). This confirms that a vacancy ordering occurs on the octahedral sites of the spinel lattice, which disappears with increasing substitution. Moreover, interesting features are observed during the high temperature transformation of these metastable γ phases into the rhombohedral α phases (*2, 3*). For the phases a linear variation of absorption frequency with chromium content was observed; this permitted an unknown compound of type α-$(Fe^{3+}_{6-y}Cr_y^{3+})O_9^{2-}$ to be identified. In certain temperature ranges and oxidation times, and during transformations the α phase composition differed from that of the corresponding γ phase. On the other hand, from the disappearance of the 635-cm^{-1} band, which is characteristic of these defect spinels, we show that the precipitation temperature of hematite from defect zinc–iron ferrites increases with the extent of substi-

0022-4596/83 $3.00

tution. For the α phases at 700°C the intensity difference of the 380- and 470-cm^{-1} absorption bands varies linearly with the percentage of α-Fe_2O_3; hence, it is possible to determine the extent of substitution in zinc-substituted magnetites.

All this calls for extension of this investigation to cobalt-substituted magnetites which also oxidize into phase γ for sufficiently small crystallite sizes. The structural changes occurring when the γ phases undergo a thermal treatment are also monitored using infrared spectroscopy.

Samples and Experimental Methods

The compounds studied were obtained by thermal decomposition of mixed iron and cobalt oxalates $(Fe_{1-x}Co_x)C_2O_4 \cdot 2H_2O$ $(0 < x < \frac{1}{3})$ and treated at low temperature (<500°C), in accordance with the conditions stated in (*4*). The crystallite size (determined from specific area and by electron microscopy) is roughly 70 nm. For $x \leq 1$, the synthesized materials form inverse spinels and have the cation distribution $(Fe^{3+})_A(Co_x^{2+}Fe_{1-x}^{2+}Fe^{3+})_BO_4^{2-}$. The Co^{2+} ions are located at the octahedral sites. Defect spinel-type cubic sesquioxides were obtained by low temperature oxidation (<300°C) of previously formed solid solutions according to the reaction

$$(Co_x^{2+}Fe_{1-x}^{2+}Fe_2^{3+})O_4^{2-} + (1-x)/4O_2^{2-} \rightarrow x(Co^{2+}Fe_2^{3+}O_4^{2-}), \tfrac{3}{2}(1-x)Fe_2^{3+}O_3^{2-}.$$

The crystallographic and magnetic studies (*5*) showed that the vacancies were positioned on octahedral sites, resulting in the structure

$$(Fe^{3+})_A(Co_x^{2+}Fe_{(5-2x)/3}^{3+}\square_{(1-x)/3})_BO_4^{2-}.$$

The lattice parameter varies linearly with rising x from 0.8345 nm for γ-Fe_2O_3 to 0.8383 nm for $CoFe_2O_4$. Finally, the morphology of these defect spinels is similar to that of the initial phases; in particular, the crystallite sizes are almost the same. The present study is not only restricted to the stability range of the γ phases but is extended to higher temperatures (>300°C) where these phases are converted to rhombohedral phase α and ferrite according to the reaction

$$(Fe^{3+})_A(Fe_{(5-3x)/3}^{3+}Co_x^{2+}\square_{(1-x)/3})_BO_4^{2-} \rightarrow xCoFe_2O_4 + \tfrac{4}{3}(1-x)Fe_2O_3.$$

The position, width, and shape of ir absorption lines of powder samples depend on size and shape of the crystallites (*6*); the samples consist of almost spherical grains with an average diameter in the range between 60 and 80 nm. The spectra were measured at room temperature using a Perkin–Elmer model 580B double beam spectrophotometer over the range 800–200 cm^{-1}; the reference beam attenuation was changed in order to obtain the best features in each region. The use of TlBr pellets (in an attempt to match indices of refraction of sample and medium) did not significantly improve the quality of the results and all ir spectra shown below were derived from CsI pellets and are normalized to 4 μmole of sample/200 mg CsI. An absolute absorbance calibration was made using a precalibrated screen, and the peak heights are accurate to within 5 to 10%. The wavenumber accuracy was ± 1 cm^{-1} for 800–500 cm^{-1} and ± 2 cm^{-1} for the region 500–250 cm^{-1}. The different oxidations (vs time and vs temperature) were performed in a Setaram MTB 10-8 microbalance.

Results and Discussions

1. Initial phases $(Fe^{3+})_A(Co_x^{2+}Fe_{1-x}^{2+}Fe^{3+})_BO_4^{2-}$

In the region under study the ir spectra of the initial inverse spinels have two absorption bands ν_1 and ν_2 which for magnetites ($x = 0$) occur at 570 and 370 cm^{-1} and for $CoFe_2O_4$ ($x = 1$) at 590 and 383 cm^{-1} (Fig.

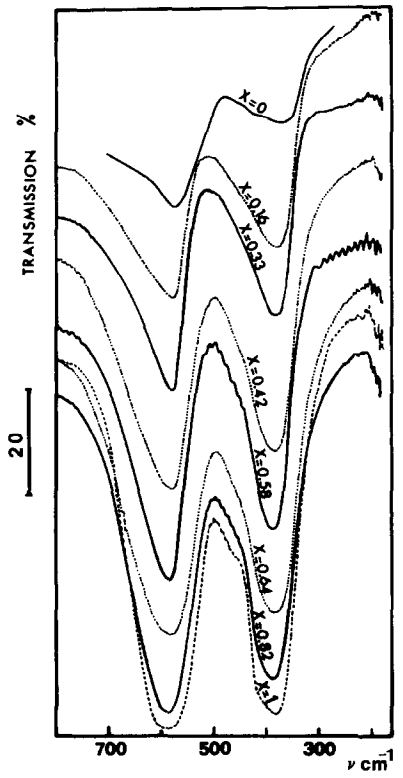

FIG. 1. Infrared spectra of $(Fe^{3+})_A(Fe^{3+}Fe^{2+}_{1-x}Co^{2+}_x)_BO^{2-}_4$ spinels.

1). Ferrites possess the structure of mineral spinel that crystallizes in the cubic form with space group $Fd3m$-O^7_h. Using the space group and point symmetries, group theoretical calculations show the existence of four ir active fundamentals (T_{1u}) in the vibrational spectra of normal as well as inverse cubic spinels (*7, 8*). However, interactions may always occur between the four ir active modes because they belong to the same representation T_{1u} (*9*). The question becomes still more complex for inverse spinels such as Fe_3O_4 and $CoFe_2O_4$ where cations with different valenc are on the same type of site and hence disturb local symmetry. For the ir absorption spectrum study of solid solutions $(M,Fe)_3O_4$, Ishii *et al.* (*10*) calculated the optically active lattice vibrations of Fe_3O_4. They assigned the band corresponding to frequency ν_1 at 570 cm^{-1} to the $\nu_1(T_{1u})$ mode, which is the Fe–O stretching mode of the tetrahedral and octahedral sites; they assigned the band corresponding to frequency ν_2 at 370 cm^{-1} to the $\nu_2(T_{1u})$ mode which is a Fe–O stretching mode for octahedral sites. The bands related to the $\nu_3(T_{1u})$ and $\nu_4(T_{1u})$ modes were assigned by these authors to the motion of Fe ions on the tetrahedral sites against those of octahedral sites, and to an O–Fe–O bending mode of the tetrahedral and octahedral sites, respectively. These bands, which are expected to be weak (*10*), have not been observed down to 50 cm^{-1}.

For cobalt-substituted magnetites in the $Fd3m$ spinel structure (*5, 11*), Co^{2+} ions as well as Fe^{3+} ions are present in octahedral sites and the increase in cobalt concentration increases the Co^{2+}–O^{2-} complexes. Thus, when iron is substituted by cobalt, whereas the tetrahedral cations remain the same, all bands shift towards high frequencies, indicating a major contribution of the octahedral cations to these vibrational modes. Tarte (*12*) also observed that in ferrites both bands depend on the nature of octahedral cations, and, to a lesser extent, on the tetrahedral ions. Comparing this result with the spectrum of zinc-substituted magnetites of the same composition but with the cation distribution $(Zn^{2+}_xFe^{3+}_{1-x})_A(Fe^{2+}_{1-x}Fe^{3+}_{1+x})_BO^{2-}_4$, we have interpreted (*3*) the shift of the high-frequency band (ν_1) towards the long-wavelength range (from 570 to 552 cm^{-1}). This arises quite naturally from the fact that when Zn^{2+} displaces Fe^{3+} ions from tetrahedral sites the effective mass of these complexes is increased. Thus, the value of the elastic bond constants is increased and the frequency of the intrinsic vibrations of these complexes is decreased.

The two broadened bands observed for low cobalt-substitution extents are typical of both a disordered inverse spinel (with two diffuse bands) and a solid compound containing mobile electrons, responsible for

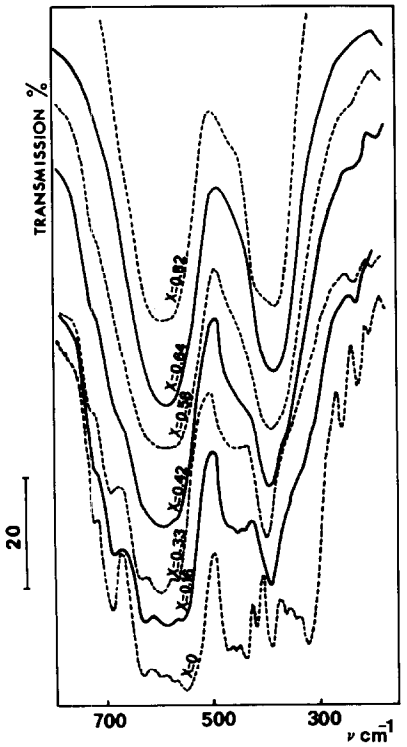

FIG. 2. Infrared spectra of defect $(Fe^{3+})_A(Co_x^{2+}Fe_{(5-2x)/3}^{3+}\square_{(1-x)/3})_BO_4^{2-}$ spinels.

the continuous absorption coinciding with the vibrational absorption.

2. *Lacunar phases* $(Fe^{3+})_A(Co_x^{2+}Fe_{(5-2x)/3}^{3+}\square_{(1-x)/3})_BO_4^{2-}$

For $x < 0.40$, the spectrum of the γ phases obtained by oxidizing the previous phases at 300°C is complicated (Fig. 2); we have shown (*13*) that this complexity, which is highly abnormal for a spinel, may be explained by an ordering of vacancies and cations on octahedral sites. However, cobalt in octahedral sites has a marked deleterious influence on the type of ordering process when compared to defect phases of type $(Zn_x^{2+}Fe_{1-x}^{2+})_A(Fe_{(5+x)/3}^{3+}\square_{(1-x)/3})_BO_4^{2-}$ where the bivalent cation is preferentially located on the tetrahedral sites. Figure 3 shows that for the same extent of substitution (for example, $x = 0.16$) presence of Co can cause the 365-, 326-, 311-, and 260-cm^{-1} absorption bands to disappear. Also the ordering process strongly depends on the presence of the foreign cation on octahedral sites. This influence is also evident from the study of the partially oxidized magnetites $(Fe^{3+})_A(Fe_{1+2\delta}^{3+}Fe_{1-3\delta}^{2+}\square_\delta)_BO_4^{2-}$ with $0 < \delta < \frac{1}{3}$ and $\delta = (1 - x)/3$ where, for an oxidation ratio $\delta = 0.28$ (the three samples have the same number of vacancies $\square$ on octahedral sites), we have encountered a large number of absorption bands, specially in the region 370–260 cm^{-1} (Fig. 3). This fine structure corresponds to an ordering of the vacant sites in the γ phase. For ordered spinel-type compounds, White and De Angelis (*14*) have determined the number of active modes. This number increases considerably when ordering takes place on octahedral or tetrahedral sites; thus, for the 1 : 1 or 1 : 3 ordering on octahedral sites the number of

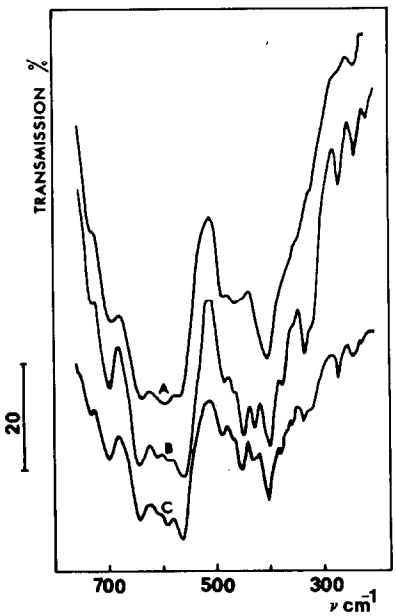

FIG. 3. Comparison of infrared spectra of defect spinels with the same number of vacancies ($x = 0.16$). A: $(Fe^{3+})_A(Co_{0.16}^{2+}Fe_{1.56}^{3+}\square_{0.26})_BO_4^{2-}$. B: $(Zn_{0.16}^{2+}Fe_{0.84}^{3+})_A(Fe_{1.72}^{3+}\square_{0.28})_BO_4^{2-}$. C: $(Fe^{3+})_A(Fe_{1.56}^{3+}Fe_{0.16}^{2+}\square_{0.28})_BO_4^{2-}$.

active modes is 31 (for the space group D_4^3 – P_{4_122}) and 21, respectively.

The X-ray powder diagram of these compounds exhibits prominent spinel reflections as well as a fairly large number of peaks which are generally weak or very weak. This suggests the possibility of two ordering schemes:

(1) reflections which are forbidden in the space group of conventional spinels but allowed in the case of a cubic cell with a 3 : 1 order (belonging to group $O^7 - P_{4_132}$). The γ phases substituted by cobalt with $x < 0.40$ exhibit a number of superstructure lines which are easily indexed using a primitive cubic cell with $a = 0.8347$ nm for $x = 0.16$.

(2) reflections which can only be accounted for by assuming a square cell with a ratio $c/a = 3$. As already discussed in a previous paper (*15*), the X-ray diffraction pattern of γ-Fe_2O_3 (space group $P_{4_12_12}$) corresponds to a tetragonal configuration with $a = 0.835$ nm and $c = 2.50$ nm. The X-ray diffraction patterns of the γ phase substituted by zinc and partially oxidized magnetite are similar to that reported for the tetragonal γ-Fe_2O_3. This observation has also been confirmed by transmission electron microscopy (*16*). These γ defect phases possess an ordered arrangement of cation vacancies with a period of $\frac{1}{3}$ unit vector along the [100] and [010] direction for the composition $(Zn_{0.18}^{2+}Fe_{2.54}^{3+}\square_{0.28})O_4^{2-}$.

Comparing this result with the spectrum of the γ phase containing substituted cobalt, a number of superstructure lines of very weak intensity have not been observed and the ir spectrum contains no band below 390 cm^{-1}, suggesting a different arrangement of vacancies and cations on octahedral sites—probably a 3 : 1 ordered distribution.

For $x > 0.40$, the bands of weak intensity disappear progressively (the bands at 474, 691, and 720 cm^{-1}) (Fig. 2) and the spectrum is slightly different from that of the initial phase of the same composition x, with the total disappearance of vacancy ordering. This is consistent with the absence of superstructure reflexions in the X-ray diagram.

3. Precipitation of α-Fe_2O_3 from Defect Phases

If the defect phases γ of different compositions for $x < 0.60$ are heated for more than 4 hr at 760°C, the spectrum exhibits (Fig. 4) the characteristic bands of α-Fe_2O_3 at 591, 542, 470, 379, 330, and 230 cm^{-1}. This correlates quite well with the data published for α-Fe_2O_3 obtained by heating goethite (*6*) where from factor group analysis (*17*) six vibrations, of which four are doubly degenerate, are predicted to be active in the ir spectrum. As the extent of substitution was increased, the ir spectra revealed the pro-

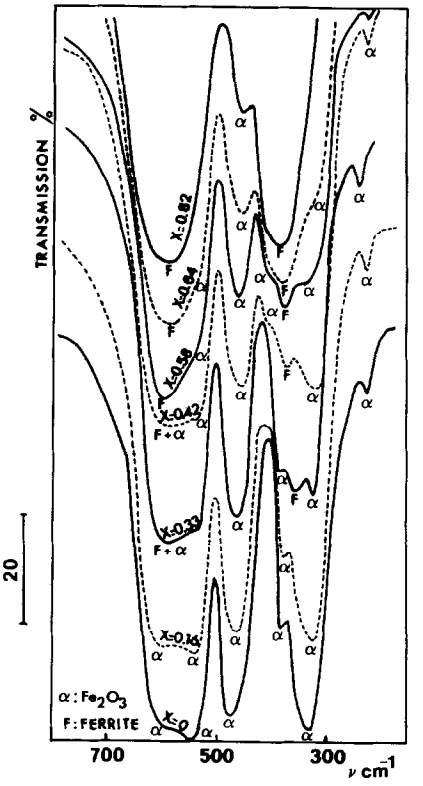

FIG. 4. Infrared spectra of α-Fe_2O_3 + $CoFe_2O_4$.

gressive disappearance of the absorption peaks at 591, 542, 379, and 330 cm^{-1} (these bands were observed as a shoulder) and close to 350–380 cm^{-1} a small band with low intensity appeared which is attributed to $CoFe_2O_4$. Finally, for $x = 1$, the ir spectrum shows two intense absorption bands at 590 and 383 cm^{-1}, due to the ferrite phase. These results show that the best choice of frequencies for identification α-Fe_2O_3 is the strong band at 470 cm^{-1}. Moreover, over the range examined, the α-Fe_2O_3 peak at 379 cm^{-1} disappeared for $x > 0.60$ and another peak appeared close to 350–380 cm^{-1}. To demonstrate systematic changes in spectra to α-Fe_2O_3 : ferrite variations, the intensity difference between the $390_{\alpha\text{-}Fe_2O_3}$- and $470_{\alpha\text{-}Fe_2O_3}$-$cm^{-1}$ band ($x < 0.60$) and the $385_{ferrite}$- and $470_{\alpha\text{-}Fe_2O_3}$-$cm^{-1}$ band ($x > 0.60$) versus x is exhibited in Fig. 5. This figure shows that the intensity difference linearly decreases as the extent of substitution increases, then reaches a minimum at $x = 0.52$, and thereafter linearly increases. For zinc-substituted defect spinels the minimum observed in Fig. 5 shifts towards greater substitution ($x = 0.90$). Based upon these systematic spectral variations it would seem, at first, quite simple to determine the unknown degree of substitution for a zinc- or cobalt-substituted magnetite. Moreover, this minimum, which is attributable to the formation of the ferrite phase, seems to be characteristic of the divalent cation.

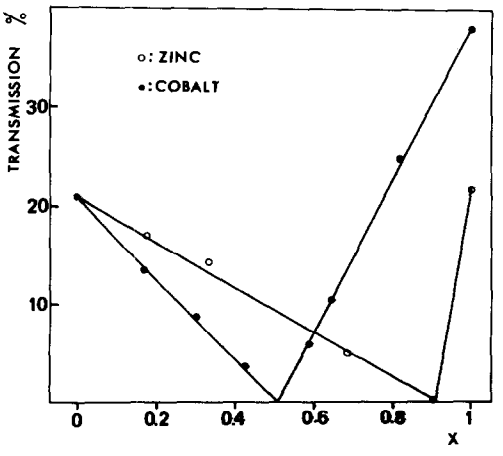

FIG. 5. Variation of the intensity difference of the bonds 390–385 and 470 cm^{-1} as a function of extent of substitution.

4. Variation of the Infrared Spectrum with Temperature and Oxidation Time of the γ Phase

At temperatures below 760°C but above the oxidation temperature for formation of the γ phase (300°C), the conversion $\gamma \rightarrow \alpha$ occurs progressively at any composition. This is indicated as a function of temperature for a given oxidation time (Figs. 6 and 7) or as a function of time for the same temperature. Quite different variations in the absorption occur during oxidation. In all

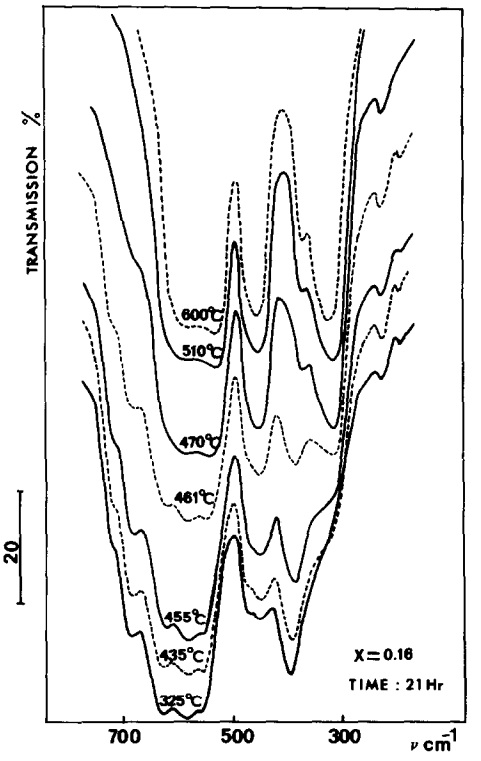

FIG. 6. Variation with temperature of the ir spectrum of the γ defect phase of composition $x = 0.16$.

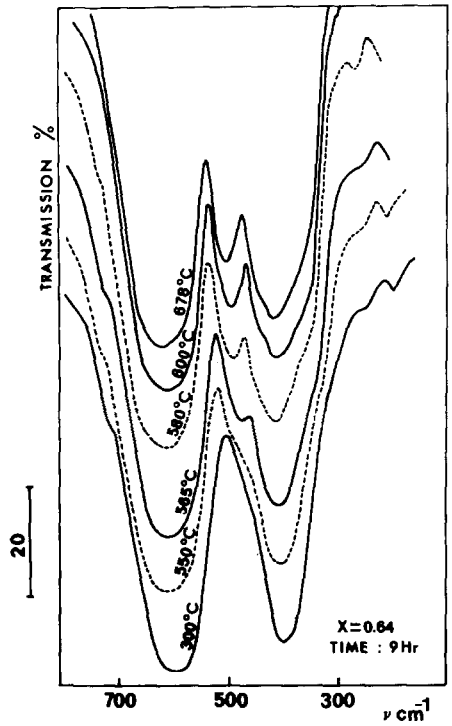

FIG. 7. Variation with temperature of the ir spectrum of the γ defect phase of composition $x = 0.64$.

cases, when the temperature was increased (or the time at constant temperature), the 720-cm^{-1} peak of the γ phase which occurred as a shoulder of relatively low intensity disappeared; also, the 470-cm^{-1} peak assigned to α-Fe_2O_3 gradually became more intense. It is thus possible, for example, by fixing the oxidation time, to evaluate a transition temperature for each composition, by noting the temperature T_B at which the 470-cm^{-1} peak appears or to the temperature T_E at which the 720-cm^{-1} shoulder disappears. Figure 8 shows the temperatures T_B and T_E at the beginning and the end of each transformation versus composition x, as well as the temperature T_M as related to $(T_B + T_E)/2$. In all cases the variation of the transition temperature with x points to an increase in stability of these γ defect phases with the increase of cobalt substitution. This temperature T_M is close to the transformation temperature as obtained by electrical conductivity (*18*). An increase in the temperature of precipitation as caused by the decrease in α-Fe_2O_3 concentration might be closely associated with the cation vacancy in the spinel lattice; for, homogeneous oxidation of ferrous ferrites generates cation vacancies whose concentration is proportional to the α-Fe_2O_3 content. Similar results have been noted (*2, 19*) for zinc-substituted defect spinels. The effect of divalent cations on the precipitation of hematite from defect phases γ is most pronounced

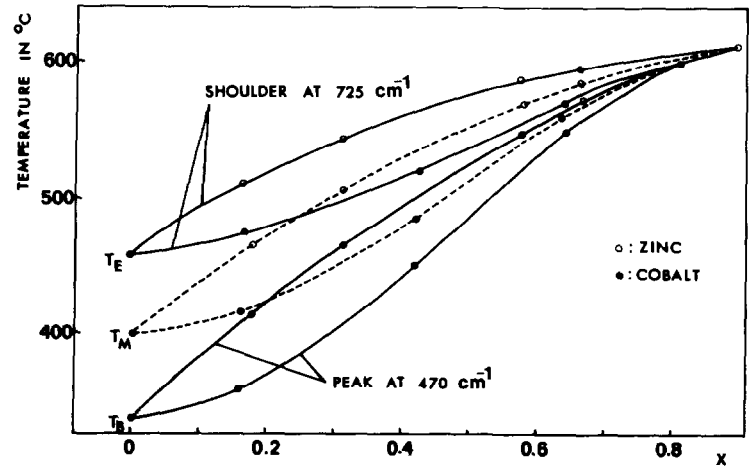

FIG. 8. Effect of composition x on temperature of precipitation.

for Zn, and cation distribution rather than ionic radius may explain the different temperatures of hematite precipitation. This is because the transformation does appear to involve a restacking due to short-distance movements of atoms (*20*). Thus Zn ions in tetrahedral sites of the spinel structure hinder the precipitation of hematite because Zn ions are strongly bound by covalent bonds, in contrast to the ionic bonding of Co^{2+} ions on octahedral sites.

Conclusion

This work has shown that the different steps of oxidation of cobalt-substituted magnetites can be identified through their characteristic ir absorption. In contrast to the defect phase γ substituted by zinc or partially oxidized magnetites no perfectly ordered γ phase has been obtained for $x < 0.30$, as the ordering of vacancies is a function of the foreign cation in octahedral sites. For $x > 0.30$, the fine structure disappears and the ir spectrum exhibits two broadened bands characteristic of a disordered phase. If the metastable phase γ is heated for more than 1 hr at 750°C, the spectrum exhibits bands of the α-Fe_2O_3 and of the ferrite phase. At any temperature lower than 600°C this transformation $\gamma \rightarrow \alpha$ occurs very slowly; it is then possible to determine a transformation temperature for each composition, which increases with cobalt substitution x. In addition, since the intensity difference between the bands 390–380 and 470 cm^{-1} varies linearly with x, a composition of the unknown can be determined.

References

1. B. GILLOT, F. BOUTON, J. F. FERRIOT, F. CHASSAGNEUX, AND A. ROUSSET, *J. Solid State Chem.* **21,** 375 (1977).
2. B. GILLOT, R. M. BENLOUCIF, AND A. ROUSSET, *J. Solid State Chem.* **39,** 329 (1981).
3. B. GILLOT, F. BOUTON, F. CHASSAGNEUX, AND A. ROUSSET, *J. Solid State Chem.* **33,** 245 (1980).
4. P. MOLLARD, A. COLLOMB, J. DEVENYI, A. ROUSSET, AND J. PARIS, *IEEE Trans. Magn.* **11,** 894 (1975).
5. A. ROUSSET, P. MOLLARD, AND A. GIRAUD, *C.R. Acad. Sci. Paris Ser. C* **275,** 709 (1972).
6. C. J. SERNA, J. L. RENDON, AND J. E. EGLESIAS, *Spectrochim. Acta Part A* **38,** 797 (1982).
7. R. D. WALDRON, *Phys. Rev.* **99,** 1727 (1955).
8. S. HAFNER, *Z. Kristallogr.* **115,** 331 (1961).
9. J. PREUDHOMME, *in* "Séminaire de Chimie de l'Etat Solide" (J. P. Suchet, Ed.), p. 32, Masson, Paris, 1974.
10. M. ISHII, M. NAKAHIRA, AND T. YAMANAKA, *Solid State Commun.* **11,** 209 (1972).
11. O. S. JOSYULU AND J. SOBHANADRI, *Phys. Status Solidi A* **59,** 323 (1980).
12. P. TARTE, *Spectrochim. Acta* **19,** 49 (1963).
13. B. GILLOT AND F. BOUTON, *J. Solid State Chem.* **32,** 303 (1980).
14. W. B. WHITE AND B. A. DE ANGELIS, *Spectrochim. Acta Part A* **23,** 985 (1967).
15. B. GILLOT, A. ROUSSET, AND G. DUPRE, *J. Solid State Chem.* **25,** 263 (1978).
16. B. GILLOT, R. M. BENLOUCIF, J. C. MUTIN, AND A. ROUSSET, *C.R. Acad. Sci. Paris* (to be published).
17. J. D. H. DONNAY AND G. TURRELL, *Chem. Phys.* **6,** 1 (1974).
18. B. GILLOT, R. M. BENLOUCIF, AND F. JAMMALI, *Mater. Chem. Phys.* (1983).
19. B. GILLOT, R. M. BENLOUCIF, AND A. ROUSSET, *Phys. Status Solidi A* **65,** 205 (1981).
20. B. GILLOT, *Mater. Res. Bull.* **13,** 783 (1978).